Environmental Science & Technology

Article

pubs.acs.org/est

Spatial and Temporal Trends in Lake Erie Hypoxia, 1987−2007

Yuntao Zhou,*[,†,‡] Daniel R. Obenour,[‡,§] Donald Scavia,[‡,§,∥] Thomas H. Johengen,[⊥] and Anna M. Michalak[†]

[†]Department of Global Ecology, Carnegie Institution for Science, Stanford, California 94305, United States

[‡]Department of Civil and Environmental Engineering, University of Michigan, Ann Arbor, Michigan 48109, United States

[§]School of Natural Resources and Environment, University of Michigan, Ann Arbor, Michigan 48109, United States

[∥]Graham Sustainability Institute, University of Michigan, Ann Arbor, Michigan 48103, United States

[⊥]Cooperative Institute for Limnology and Ecosystems Research, School of Natural Resources and Environment, University of Michigan, Ann Arbor, Michigan 48109, United States

Supporting Information

ABSTRACT: Hypoxic conditions, defined as dissolved oxygen (DO) concentrations below 2 mg/L, are a regular summertime occurrence in Lake Erie, but the spatial extent has been poorly understood due to sparse sampling. We use geostatistical kriging and conditional realizations to provide quantitative estimates of the extent of hypoxia in the central basin of Lake Erie for August and September of 1987 to 2007, along with their associated uncertainties. The applied geostatistical approach combines the limited in situ DO measurements with auxiliary data selected using the Bayesian Information Criterion. Bathymetry and longitude are found to be highly significant in explaining the spatial distribution of DO, while satellite observations of sea surface temperature and satellite chlorophyll are not. The hypoxic extent was generally lowest in the mid-1990s, with the late 1980s (1987, 1988) and the 2000s (2003, 2005) experiencing the largest hypoxic zones. A simple exponential relationship based on the squared average measured bottom DO explains 97% of the estimated variability in the hypoxic extent. The change in the observed maximum extent between August and September is found to be sensitive to the corresponding variability in the hypolimnion thickness.

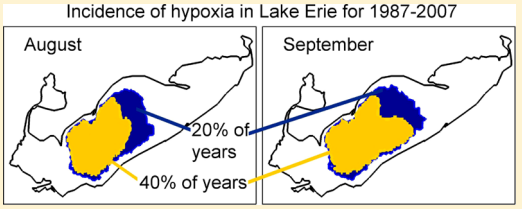

1. INTRODUCTION

Summer hypoxia is a natural phenomenon in the central basin of Lake Erie, probably dating back thousands of years.[1] However, evidence suggests that oxygen depletion rates increased in the 1950s due to anthropogenic factors.[2] During summer, the strong vertical thermal gradient (i.e., stratification) reduces mixing and hence the flux of oxygen into the hypolimnion, where low light restricts photosynthesis. Decomposing phytoplankton and other settled organic matter consume oxygen, often reducing it to below the 2 mg/L hypoxic threshold in the hypolimnion.

Hypoxic areal extent is an important indicator for tracking historical changes in water quality, and is often used as a response metric for water quality management.[3] However, because of sparse sampling, the spatial and temporal dynamics of hypoxia in Lake Erie are poorly understood. Various models have been used to estimate the extent of hypoxia in Lake Erie. Although one-dimensional[4] and box water quality models[5−7] have been used to describe temporal dissolved oxygen (DO) dynamics, these are not well suited for assessing the hypoxic spatial extent. Multisegment box models for Lake Erie have provided estimates of the spatial distribution of DO, but their spatial resolution is rather coarse. Burns et al.[8] used linear interpolation to estimate the maximum yearly extent of hypoxia in the central basin of Lake Erie for 1983 to 2002 using the yearly minimum observed DO for each of ten regular sampling stations. Although simple techniques such as linear and nonlinear interpolation[9,10] and inverse distance weighted interpolation[11] can provide an estimate of spatial extent, they do not rigorously account for the spatial correlation of the data, do not provide quantitative estimates of uncertainties, and generally cannot make use of auxiliary variables to improve estimates.

Herein, we used the Bayesian Information Criterion (BIC),[12] implemented within a geostatistical regression framework,[13,14] to identify a set of auxiliary variables that inform the distribution of DO in the central basin of Lake Erie. We then applied Universal Kriging (UK; a.k.a. kriging with an external drift) and conditional realizations[15] to assess the spatial distribution of DO using both the available DO observations and the identified auxiliary data. These methods made it possible to provide a detailed history of late-summer hypoxic extent in Lake Erie from 1987 to 2007, to provide a rigorous and quantitative assessment of associated uncertainty, and to identify factors that correlate with this variability. This new

Received: August 22, 2012
Revised: December 3, 2012
Accepted: December 13, 2012
Published: December 13, 2012

historical data set was then used to explore the impact of stratification dynamics on intraseasonal changes in hypoxic extent, and to develop a simple model of hypoxic extent based on the average measured bottom water DO concentration.

2. DATA DESCRIPTION AND EXAMINED CASE STUDIES

Dissolved Oxygen. The in situ DO data used in this study were collected by the U.S. EPA Great Lakes National Program Office (GLNPO),[16] the National Water Research Institute of Environment Canada (NWRI),[4] and the National Oceanic and Atmospheric Administration (NOAA) Great Lakes Environmental Research Laboratory (GLERL). GLNPO and NWRI have been collecting DO data in April, August, September, and October since the 1980s at ten fixed stations in the central basin of Lake Erie (Figure S1, Tables S1 and S2 in the Supporting Information).[17] In addition, GLERL collected DO measurements at approximately 60 locations in the central basin of Lake Erie from May through October in 2005 and approximately 40 locations in the central basin in September 2007 as part of the International Field Years on Lake Erie (IFYLE) program.[18] Overall, the analysis presented here was based on 75 sampling cruises for August and September between 1987 and 2007 (Tables S1 and S2), 61 of which detected hypoxia. Note that within this study period, no DO data are available for August 1992, 1994, and 1995 or for September 1991, 2000, and 2006.

At each sampling location, DO concentrations were measured at about 3-, 1-, and <1-m vertical intervals throughout the water column for the GLNPO, NWRI, and GLERL cruises, respectively. For our analysis, we used the DO observations 1 or 2 m above the lake bottom at each sampling location (depending on the deepest available observations), which are normally representative of the DO concentration in the hypolimnion. The focus of our study was on August and September, the months when the hypoxic extent is typically at its maximum.[19] We also restricted our analysis to the central basin of Lake Erie, the basin most susceptible to hypoxia due to its depth and nutrient loading.[4]

Auxiliary Data. To augment the sparse in situ DO measurements, auxiliary variables with full spatial coverage were considered in the analysis. These variables, chosen based on availability and expected associations with DO, included latitude, longitude, bathymetry, and satellite-derived monthly average sea surface temperature (SST) and surface chlorophyll concentration from April to September. The bathymetry data are a subset of the New Bathymetry of Lake Erie and Lake St. Clair from the NOAA National Geophysical Data Center.[20] The chlorophyll data are derived from the Sea-viewing Wide Field-of-view Sensor (SeaWiFS), and are available from the National Aeronautics and Space Administration (NASA) Ocean Color Web facility[21] at a resolution of 9 km × 9 km for 1998 onwards. SST data at 2.5 km × 2.5 km are available starting in 1992 from Great Lakes Surface Environmental Analysis (GLSEA),[22] a digital map of the Great Lakes surface temperature and ice cover produced daily from Advanced Very High Resolution Radiometer (AVHRR) data by NOAA GLERL. These GLSEA data are produced specifically for the Great Lakes using a smoothing algorithm.[23] All data were regridded to a 2.5 km × 2.5 km resolution using nearest neighbor interpolation.

Analyzed Cases. Because satellite data are not available for the entire study period, we designed and compared two case studies. Case 1 covered 1987 to 2007, and used only bathymetry, latitude, and longitude as auxiliary variables. Case 2 included these variables, plus the GLSEA SST and SeaWiFS chlorophyll data for April through September, and covered 1998 to 2007.

3. METHODOLOGY

This section describes the geostatistical framework for estimating the hypoxic extent for the central basin of Lake Erie.

3.1. Universal Kriging. UK uses auxiliary variables, which for the cases examined here included latitude, longitude, bathymetry, SST, and chlorophyll concentrations, in addition to the limited in situ DO measurements, to obtain a detailed spatial model of DO for the central basin of Lake Erie. UK has been widely used in the environmental sciences for applications such as estimating snow accumulation, temperature, and precipitation,[24−26] characterizing contaminant distributions,[27] and understanding emissions and uptake of carbon dioxide.[13] Within the context of hypoxia, Murphy et al.[28] used UK, among other approaches, to interpolate water quality parameters such as salinity, water temperature, and DO in the Chesapeake Bay, using the output from a water quality model as auxiliary information; and Obenour et al.[14] used a UK-type model to separate the impacts of stratification and nutrient loading on DO in the Gulf of Mexico.

The role of auxiliary variables in UK is analogous to the role of independent variables (covariates) in multiple linear regression. Contrary to linear regression, however, UK also (i) accounts for the spatial correlation (i.e., smoothness) of the DO distribution, and (ii) is an exact interpolator, such that it reproduces all the available DO observations to within their measurement error. We performed UK using data from all the cruises with hypoxic measurements simultaneously, such that the relationship between auxiliary variables and DO remained constant from cruise to cruise. The estimates of DO themselves, however, were cruise-specific, and no correlation was assumed among regression residuals from different cruises.

For each of the two examined cases, the $n \times 1$ observation vector $\mathbf{z}$ of DO is defined as:

$$\mathbf{z} = \begin{bmatrix} \mathbf{z}_1 \\ \mathbf{z}_2 \\ \vdots \\ \mathbf{z}_y \end{bmatrix} \quad (1)$$

where $\mathbf{z}_i$ (i = 1, 2, ..., y) are $n_i \times 1$ vectors of DO measurements, n_i is the number of DO measurements for the ith cruise (i.e., $n = \sum_{i=1}^{y} n_i$), and y is the total number of cruises for which DO data are used in each case (y = 61 for Case 1; y = 32 for Case 2).

Within the UK framework, the DO distribution is modeled as the sum of a deterministic term (trend) and a zero-mean stochastic term (spatially correlated residuals). The deterministic term represents the portion of the DO distribution that can be explained by the available auxiliary variables and spatially constant cruise offsets (corresponding to each cruise), and the stochastic term represents the remaining portion of the observed variability:

$$\mathbf{z} = \mathbf{X}_z\boldsymbol{\beta} + \mathbf{z}_{res} \quad (2)$$

where $\mathbf{X}_z$ is a known $n \times (y + p)$ matrix of y categorical variables (corresponding to unique offsets [i.e., intercepts] for each cruise) and p auxiliary variables, $\boldsymbol{\beta}$ is a $(y + p) \times 1$ vector of

dx.doi.org/10.1021/es303401b | Environ. Sci. Technol. 2013, 47, 899−905

unknown drift coefficients on these variables, and $\mathbf{z}_{res}$ is an $n \times 1$ vector of residuals. The approach used for selecting a subset of auxiliary variables from among those listed in Section 2 is presented in Section 3.2. Overall, the model of the trend ($\mathbf{X}_z$) is expressed as:

$$\mathbf{X}_z = \begin{bmatrix} \mathbf{1}_1 & \cdots & \phi & \mathbf{X}_1 \\ \vdots & \ddots & \vdots & \vdots \\ \phi & \cdots & \mathbf{1}_y & \mathbf{X}_y \end{bmatrix} \tag{3}$$

where $\mathbf{1}_i$ (i = 1, 2, ..., y) are $n_i \times 1$ vectors of ones, and $\mathbf{X}_i$ is an $n_i \times p$ matrix of auxiliary variables representing the trend for each cruise. Because the mean DO concentration is expected to change from cruise to cruise, $\mathbf{X}_z$ includes y columns of categorical variables (ones and zeros). The components in $\boldsymbol{\beta}$ that multiply the first y columns of $\mathbf{X}_z$ represent a constant offset in DO concentrations for each cruise.

The stochastic term ($\mathbf{z}_{res}$) is modeled as spatially correlated residuals. A spatial covariance function,[15] which quantifies the degree to which the spatial correlation between a pair of locations decays as a function of their separation distance (h), was defined as:

$$Q_{zz}(h) = \begin{cases} \sigma^2 + \sigma_Q^2, & h = 0 \\ \sigma^2 \exp\left(-\dfrac{h}{l}\right), & h > 0 \end{cases} \tag{4}$$

where σ^2 is the variance of the portion of the residual DO variability that is spatially correlated, $3l$ is the practical correlation range, and σ_Q^2 is the variance of the portion of the variability that is not spatially correlated (e.g., measurement error). These three model parameters were optimized by fitting the theoretical model (eq 4) to the empirical covariance of the residuals using nonlinear least-squares.[29] No covariance was assumed among cruises, and the overall $n \times n$ covariance matrix of the DO observations is therefore defined as:

$$\mathbf{Q}_{zz}(\mathbf{h}) = \begin{bmatrix} \mathbf{Q}_1 & \cdots & \phi \\ \vdots & \ddots & \vdots \\ \phi & \cdots & \mathbf{Q}_y \end{bmatrix} \tag{5}$$

where $\mathbf{Q}_i$ (i = 1, 2, ..., y) is an $n_i \times n_i$ covariance matrix for the residuals in each cruise, and all the $\mathbf{Q}_i$'s use the same covariance parameters (σ^2, σ_Q^2, and l).

The covariance matrix is used in the UK system of linear equations:

$$\begin{bmatrix} \mathbf{Q}_{zz} & \mathbf{X}_z \\ \mathbf{X}_z^T & 0 \end{bmatrix} \begin{bmatrix} \boldsymbol{\Lambda}^T \\ \mathbf{M} \end{bmatrix} = \begin{bmatrix} \mathbf{Q}_{zs} \\ \mathbf{X}_s^T \end{bmatrix} \tag{6}$$

where $\mathbf{Q}_{zs}$ is an $n \times m$ covariance matrix between the measurement and estimation locations obtained analogously to eq 5, the matrix $\mathbf{X}_s$ contains the same cruise-specific offsets and auxiliary variables as in ($\mathbf{X}_z$) but defined at the estimation locations, and T denotes a matrix transposition. The system of eq 6 was solved for $\boldsymbol{\Lambda}$, which is an $m \times n$ matrix of weights assigned to each observation for each estimation location, and for $\mathbf{M}$, which is a $(y + p) \times m$ matrix of Lagrange multipliers. Finally, $\boldsymbol{\Lambda}$ and $\mathbf{M}$ were used to obtain estimates of the DO distribution, and their associated uncertainties, throughout the central basin

$$\hat{\mathbf{s}} = \boldsymbol{\Lambda}\mathbf{z} \tag{7}$$

$$\mathbf{V}_{\hat{s}} = -\mathbf{X}_s\mathbf{M} + \mathbf{Q}_{ss} - \mathbf{Q}_{zs}^T\boldsymbol{\Lambda}^T \tag{8}$$

where $\hat{\mathbf{s}}$ is an $m \times 1$ vector of DO estimates, $\mathbf{V}_{\hat{s}}$ is the covariance matrix representing the covariances associated with these estimates, and $\mathbf{Q}_{ss}$ is an $m \times m$ covariance matrix between the residuals of estimates, obtained in the same way and using the same parameters as in eq 4. The square roots of the diagonal elements of $\mathbf{V}_{\hat{s}}$ are the standard deviations (i.e., estimation uncertainties) of the DO estimates. Because the thermocline always appears at depths of 15−20 m during summer,[30] and because shallower areas are usually oxygenated and rarely sampled, we constrained DO estimates for areas with depths of less than 15 m to be above the hypoxic threshold.

The best estimate of drift coefficients ($\hat{\boldsymbol{\beta}}$) of the auxiliary variables were obtained as:[15]

$$\hat{\boldsymbol{\beta}} = (\mathbf{X}_z^T\mathbf{Q}_{zz}^{-1}\mathbf{X}_z)^{-1}\mathbf{X}_z^T\mathbf{Q}_{zz}^{-1}\mathbf{z} \tag{9}$$

and their associated covariances were

$$\mathbf{V}_{\hat{\beta}} = (\mathbf{X}_z^T\mathbf{Q}_{zz}^{-1}\mathbf{X}_z)^{-1} \tag{10}$$

where the square roots of the diagonal elements of $\mathbf{V}_{\hat{\beta}}$ are the estimation uncertainties of the individual parameters, and the off-diagonal terms represent their estimated covariances.

Ordinary Kriging (OK), one of the most common geostatistical approaches, was used for comparison to the UK estimates as described in the Supporting Information.

3.2. Auxiliary Variable Selection. BIC was used to select a subset of auxiliary variables that can reliably represent the spatial distribution of DO.[13,14] BIC is based on the Bayesian factor or the posterior probability of a model,[12] and considers both the goodness of fit and the dimensionality of (i.e., the number of variables in) the model.[31] The BIC is defined as:

$$\mathrm{BIC} = -2\ln(L) + p\ln(n) \tag{11}$$

where L is likelihood of the observations. If the residuals are correlated and normally distributed, the negative natural logarithm of the likelihood becomes:[13]

$$-\ln(L) = \frac{1}{2}\ln|\mathbf{Q}_{zz}| + \frac{1}{2}\mathbf{z}^T(\mathbf{Q}_{zz}^{-1} - \mathbf{Q}_{zz}^{-1}\mathbf{X}_z(\mathbf{X}_z{}^T\mathbf{Q}_{zz}^{-1}\mathbf{X}_z)^{-1}\mathbf{X}_z^T\mathbf{Q}_{zz}^{-1})\mathbf{z} \tag{12}$$

BIC was evaluated for each possible combination/subset of auxiliary variables, and the set of variables with the lowest BIC was identified as the best model.

3.3. Conditional Realizations. UK yields estimates of DO concentrations in space, but cannot be used directly to estimate the hypoxic extent (i.e., the area where the DO concentration is below a given threshold) and its associated uncertainty. Conditional realizations (a.k.a. "*spatially consistent* Monte Carlo simulations")[15] of the DO distribution do this by providing equally likely alternative DO distributions. These realizations follow the spatial covariance ($\mathbf{Q}_{ss}$) and are consistent with all available observations.[32−34]

Each realization ($\mathbf{s}_{ci}$, $m \times 1$) was defined as:[35]

$$\mathbf{s}_{ci} = \boldsymbol{\Lambda}(\mathbf{z} - \mathbf{z}_{ui}) + \mathbf{s}_{ui} \tag{13}$$

where $\boldsymbol{\Lambda}$ is the $m \times n$ matrix of weights defined in eq 6, and $\mathbf{z}_{ui}$ ($n \times 1$) and $\mathbf{s}_{ui}$ ($m \times 1$) are unconditional realizations at measurement and estimation locations, respectively, obtained from

dx.doi.org/10.1021/es303401b | Environ. Sci. Technol. 2013, 47, 899−905

$$\begin{bmatrix} \mathbf{z}_{ui} \\ \mathbf{s}_{ui} \end{bmatrix} = \mathbf{C}^T\mathbf{u} \tag{14}$$

where $\mathbf{u}$ is an $(n + m) \times 1$ vector of normally distributed random values with zero mean and unit variance (note that a new vector $\mathbf{u}$ is generated for each realization), and $\mathbf{C}$ is the $(n + m) \times (n + m)$ matrix resulting from the Cholesky decomposition of the covariance matrix below:

$$\begin{bmatrix} \mathbf{Q}_{zz} & \mathbf{Q}_{zs} \\ \mathbf{Q}_{zs}^T & \mathbf{Q}_{ss} \end{bmatrix} = \mathbf{C}\mathbf{C}^T \tag{15}$$

Conditional realizations were generated for regions of the central basin with a depth greater than 15 m, and the hypoxic area was calculated for each realization by summing the areas with the DO concentrations below 2 mg/L. A thousand realizations were generated for each cruise, and the results were used to develop probabilistic estimates of hypoxic extent.

4. RESULTS AND DISCUSSION

4.1. Variables Explaining the Spatial Variability of DO. The selected auxiliary variables, together with the cruise-specific offsets, explained 53% of the DO variability for the 1987−2007 Case 1 data set. Consistent variable selections between Cases 1 and 2 indicate that the difference in the timespans does not affect the significance of the auxiliary variables. The estimated drift coefficients ($\hat{\boldsymbol{\beta}}$) for the selected auxiliary variables (Table 1) explain a portion of the within-cruise spatial variability, while the cruise-specific offsets (not shown) account for temporal variability in DO due to other cofactors, such as nutrient loading or circulation.[4,30] The consistency of the $\hat{\boldsymbol{\beta}}$ values between cases further confirms that the relationships between DO and the auxiliary variables are consistent for different time periods.

Table 1. Drift Coefficients ($\hat{\boldsymbol{\beta}}$) and Associated Uncertainties ($\sigma_{\hat{\beta}}$) for the Selected Auxiliary Variables for the Two Cases

case	longitude (mg/L)/degree	depth (mg/L)/m	depth^2 (mg/L)/m^2
1	1.24 ± 0.26	−1.40 ± 0.22	0.03 ± 0.006
2	1.17 ± 0.33	−1.36 ± 0.27	0.03 ± 0.007

Longitude, depth, and a quadratic depth term (i.e., depth squared) were selected through the BIC analysis as being significant for both examined cases (Table 1). Longitude was found to be positively correlated with DO, potentially acting as a proxy for phosphorus availability, which primarily enters the central basin from the west. Bathymetry was also correlated with DO, consistent with the fact that stratification is related to bathymetry (i.e., both the thermal structure and thickness of the bottom layer) in Lake Erie.[36,37] Based on the regression coefficients for depth and depth squared, the bottom water DO concentration is expected to be lowest at a station depth of around 23 m (close to the 24 m maximum depth of the central basin), all other factors being equal.

Neither of the remote sensing data sets (only available in Case 2) was found to significantly improve the model. In general, this suggests a more complex relationship between lake surface properties (SST and chlorophyll) and bottom DO. Surface conditions are likely decoupled from bottom conditions due to stratification and varying circulation patterns in the epilimnion and hypoliminion. For example, Walker and Rabalais[38] suggested that a relationship between chlorophyll and hypoxia was not observed in the Gulf of Mexico due to various physical and biological processes that confound a direct spatial correlation. In addition, the significance of chlorophyll may have been further diminished due to the quality of the satellite data product, which is known to have considerable uncertainty in the central basin.[39]

4.2. History of the Hypoxic Extent of Lake Erie. Because the two examined cases yield consistent estimates of the hypoxic extent and use the same auxiliary variables, we restrict our discussion to the extents and uncertainties determined in Case 1. The extents were derived from the conditional realizations of the DO distribution (Figure S2), and the maximum estimated hypoxic extent for August and September of each year and associated uncertainty (Figure 1a) show that the maximum extent occurs most often between late August and mid-September (Figure S2).

Results are qualitatively consistent with those of Makarewicz and Bertram,[40] as well as Hawley et al. (Figure 2).[18] Makarewicz and Bertram[40] reported that hypoxic extent decreased from the late 1980s to early 1990s as a result of the phosphorus load abatement programs, a part of the United States/Canada Great Lakes Water Quality Agreement of 1972.[41] Hawley et al.[18] subsequently reported that hypoxic extent increased and remained relatively high in the late 1990s and early 2000s, likely due to an increase in nonpoint source phosphorus loading or nutrient recycling by dreissenids (i.e., zebra and quagga mussels) that appeared in the system in the late 1980s.[42]

The smallest yearly hypoxic zones were observed in 1995 and 1996 (Figure 1a, Figure S2), but these years had only one and two cruises, respectively (Table S2). In 1995, the only available data were from mid-September. In 1996, August sampling data were available for August 2−4, followed by sampling in mid-September, and at only five locations. It is therefore possible that periods with larger hypoxic zones were missed in those years. In 2002 and 2004, for example, the hypoxic extent was also small in early August and mid-September, but was larger during the interim period (Figure S2). On the other end of the spectrum, the largest estimated hypoxic extents exceeded 9000 km^2 (nearly two-thirds of the surface area of the central basin deeper than 15 m) in early and mid-September 1987, late August 1988, early September 2003, and mid-September 2005.

For a given number of measurements, the uncertainties associated with the estimated extents are generally higher for months with larger hypoxic areas. These uncertainties (expressed as 95% confidence intervals) range from nearly zero for mid-September 2002 when hypoxia was negligible, to almost 6000 km^2 for September 1999. Months with large hypoxic extents have considerable areas with estimated DO concentrations close to the 2 mg/L hypoxic threshold, leading to the large uncertainty on the exact area that is hypoxic. Uncertainties are, as expected, higher for cruises with fewer measurements, such as for mid-September 1994, when only 5 measurements were available and the 95% confidence intervals span 7000 km^2 (Tables S1 and S2). Compared to other years with similar hypoxic extents, uncertainties for September 2005 and 2007 are smaller due to the more extensive DO measurements available for those two years through the IFYLE program by GLERL (Figure S2).

The maximum hypoxic extent and its location in August and September (Figures S3 and S4) vary from year to year. It is most common in the western and middle northern portion of

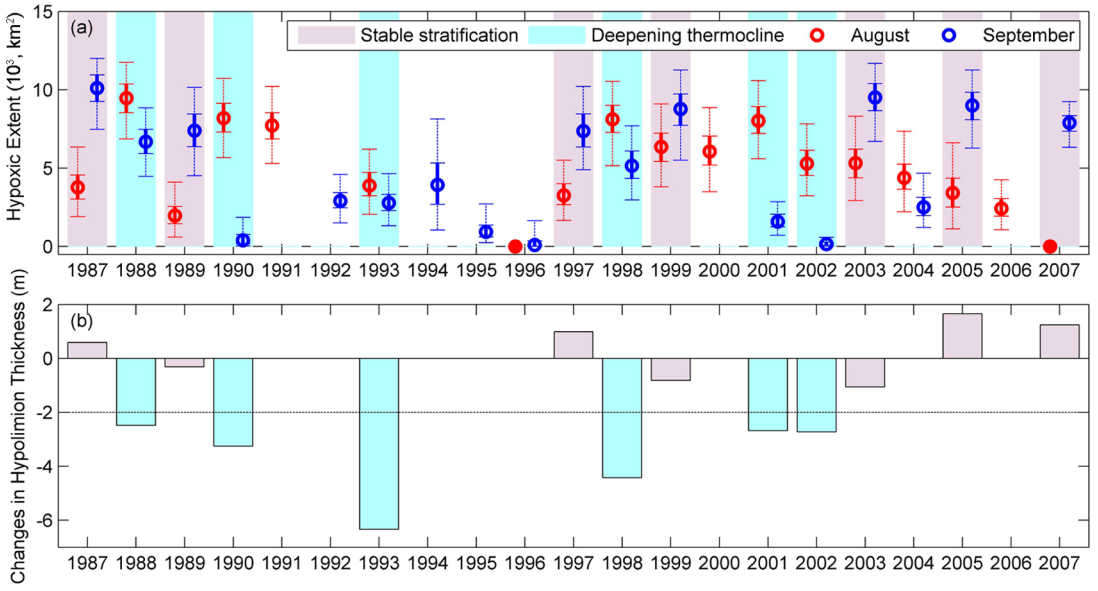

Figure 1. History of (a) the observed maximum hypoxic extent in August and September in the central basin of Lake Erie for 1987 to 2007, and (b) August to September change in hypolimnion thickness. In (a), solid circles represent months where cruises indicated no hypoxia; for months when hypoxia was observed, open circles represent the median, solid lines represent the interquartile range, and dashed lines represent the 95% confidence intervals based on the conditional realizations. Years when the August to September decrease in the hypolimnion thickness was less than 2 m (i.e., years with stable stratification) are indicated in purple in panels (a) and (b); conversely, years with a decrease of more than 2 m, corresponding to a deepening thermocline and early reoxygenation, are indicated in light blue. Data of changes in hypolimnion thickness are not available for 1996 and 2004.

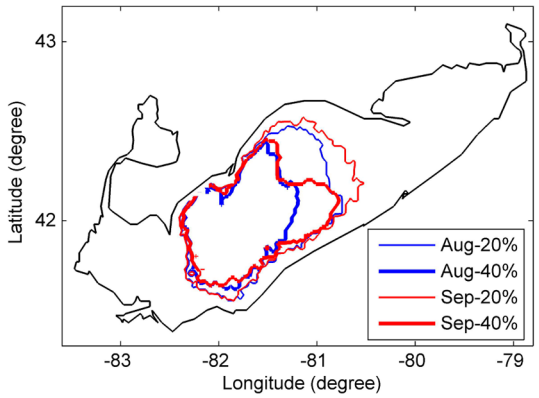

Figure 2. Areas with 20% and 40% probability of hypoxic conditions in August and September (1987 to 2007), based on estimated maximum monthly hypoxic areas (Figures S3 and S4).

the central basin in August, spreading east in September, and thus there is a greater probability of larger hypoxic areas in September relative to August (Figure 2).

Annual estimates of the maximum hypoxic extent are generally consistent with those of Burns et al.,[8] who provided the previously most complete analysis of Lake Erie hypoxia (Figure 3). Their estimates are based on a location-by-location selection of observation with the lowest DO throughout each year. One would expect that using the lowest measured concentration (especially from different times and different locations) would tend to overestimate the maximum extent of hypoxia. In addition, the lack of information from auxiliary variables makes it difficult to represent DO distributions given the very limited number of in situ DO observations, as seen by a comparison of UK and OK estimates (Figures S5 and S6). A quantitative or probabilistic comparison was not possible because Burns et al.[8] did not include actual values of hypoxic area or its uncertainty. Nonetheless, the estimates presented here are qualitatively consistent with Burns et al.,[8] supporting the notion that central basin hypoxia was more extensive in the late 1980s and late 1990s compared to the early 1990s.

4.3. Relationship of Areal Extent to Average Bottom DO Concentration at the Regular Stations and to Thermocline Depth. The estimates of hypoxic extent presented above were based on a sequential application of BIC, UK, and conditional realizations. Based on these results, we developed a simple exponential relationship for predicting hypoxic extent using the square of the average measured DO from the ten regular sampling locations (Figure 4, Figure S1). This model explains 97% of the variability in these estimated hypoxic extents:

$$E = 9.30\exp(-DO_m^2/7.09) \quad (16)$$

where E is hypoxic extent (10^3 km^2) and DO_m is the mean of the DO concentration (mg/L) across the ten sites with regular observations (Figure S1). The two model parameters were obtained through a least-squares fit to the estimated hypoxic extent from all conditional realizations, and therefore account for the varying uncertainty of the estimates across individual cruises. The ten regular sampling locations could be used as index stations for obtaining estimates of hypoxic extent for times when detailed analyses such as the one presented are not done.

During the sampling cruises, vertical temperature profile data were also collected, allowing us to analyze our results relative to the thermal structure of the lake. We found that the change in hypolimnion thickness (a correlate for thermocline depth) from August to September (Figure 1b) is an important predictor of seasonal change in hypoxic extent. For each month, the hypolimnion thickness was determined by averaging the measured hypolimnion thickness across monitoring stations for the cruise with the maximum observed hypoxic extent.

dx.doi.org/10.1021/es303401b | Environ. Sci. Technol. 2013, 47, 899−905

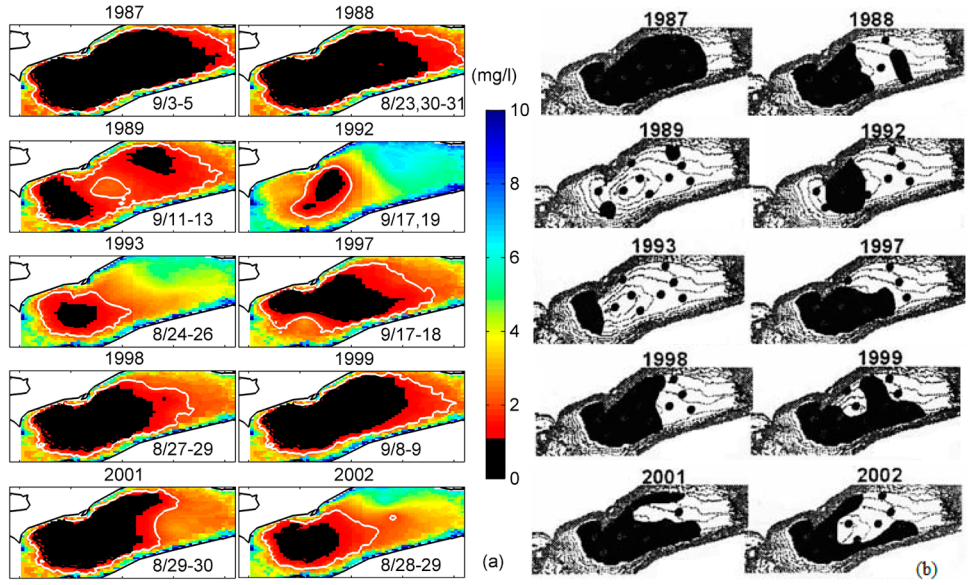

Figure 3. Comparison of (a) estimates from this study to (b) estimates from Burns et al.[8] In panel (a), white contours represent the 2 mg/L boundary, while areas with estimated concentrations below 1 mg/L are presented in black for consistency with Burns et al.[8] Subplots in (a) are based on the largest observed hypoxic zone for a given year (Figure S2).

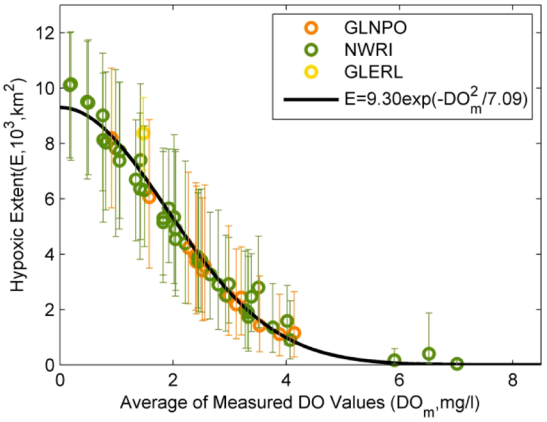

Figure 4. Predicted hypoxic extent based on average DO concentration from the ten index sampling locations and eq 16 (R^2 = 0.97). GLNPO, NWRI, and GLERL data are those from Figure S2, Tables S1 and S2, together with 95% confidence intervals.

Substantial deepening of the thermocline between August and September, as indicated by a decrease in hypolimnion thickness of more than 2 m, is associated with early reoxygenation of the basin, and a corresponding decrease in the hypoxic extent. This decrease in hypoxic extent is statistically significant for four of the six such years for which DO data were available in both August and September ($p \cong 0$ for 1990, 2001, 2002; $p = 0.05$ for 1988; $p = 0.06$ for 1998; $p = 0.18$ for 1993). Conversely, a smaller change in the hypolimnion thickness is consistent with more stable stratification and an expansion of hypoxic extent between August and September. This expansion is significant for six of the seven such years ($p \cong 0$ for 1987, 1989, 2007; $p = 0.01$ for 1997, 2005; $p = 0.02$ for 2003; $p = 0.13$ for 1999). This finding illustrates the importance of timing and thermal structure on the size of the hypoxic zone; and these factors should be considered (along with biological drivers, e.g., nutrient stimulated productivity) when exploring the inter-annual variability of hypoxia in Lake Erie.

■ ASSOCIATED CONTENT

Supporting Information

(S1) Locations of regular dissolved oxygen (DO) sampling, (S2) hypoxic extent for August and September, 1987−2007, (S3) estimated DO concentrations in August and September from the cruise with the observed maximum hypoxic extent from 1987 to 2007, and (S4) comparison of Universal Kriging (UK) results to Ordinary Kriging (OK) results. This information is available free of charge via the Internet at http://pubs.acs.org.

■ AUTHOR INFORMATION

Corresponding Author

*E-mail: ytzhou@umich.edu; phone: (734) 709-3253; fax: (650) 462-5968.

Notes

The authors declare no competing financial interest.

■ ACKNOWLEDGMENTS

This material is based upon work supported by National Science Foundation under Grant 0644648. Additional support for D.S. was provided by the NOAA Center for Sponsored Coastal Ocean Research grant NA07OAR432000. This is Ecofore Lake Erie publication 12-007. We thank Stuart Ludsin for contributing to the collection of the GLERL data, and Nathan Hawley and Anne Clites for providing the access to these data. We also thank Daniel Rucinski for helping us to obtain the Environment Canada data.

■ REFERENCES

(1) Delorme, L. D. Lake Erie Oxygen - The Prehistoric Record. *Can. J. Fish. Aquat. Sci.* **1982**, *39* (7), 1021−1029.

(2) Committee on Environment and Natural Resources. *Scientific Assessment of Hypoxia in U.S. Coastal Waters*; Interagency Working Group on Harmful Algal Blooms, Hypoxia, and Human Health of the Joint Subcommittee on Ocean Science and Technology: Washington, DC, 2010; p 154.

(3) Rabalais, N. N.; Turner, R. E.; Scavia, D. Beyond science into policy: Gulf of Mexico hypoxia and the Mississippi River. *Bioscience* **2002**, *52* (2), 129−142.
(4) Rucinski, D. K.; Beletsky, D.; DePinto, J. V.; Schwab, D. J.; Scavia, D. A simple 1-dimensional, climate based dissolved oxygen model for the central basin of Lake Erie. *J. Great Lakes Res.* **2010**, *36* (3), 465−476.
(5) Chapra, S. C. Applying Phosphorus Loading Models to Embayments. *Limnol. Oceanogr.* **1979**, *24* (1), 163−168.
(6) DiToro, D. M.; Connolly, J. P. *Mathematical Models of Water Quality in Large Lakes, Part 2: Lake Erie*; Report No. EPA-600/3-80-065; report to Large Lakes Research Station, ERL-Duluth: Grosse Ile, MI, 1980.
(7) Vollenweider, R. A. Concept of Nutrient Load as a Basis for the External Control of the Eutrophication Process in Lakes and Reservoirs. *Z. Wasser- Abwasser-Forsch.* **1979**, *12* (2), 46−56.
(8) Burns, N. M.; Rockwell, D. C.; Bertram, P. E.; Dolan, D. M.; Ciborowski, J. J. H. Trends in temperature, Secchi depth, and dissolved oxygen depletion rates in the central basin of Lake Erie, 1983−2002. *J. Great Lakes Res.* **2005**, *31*, 35−49.
(9) Hagy, J. D., III; Murrell, M. C. Susceptibility of a northern Gulf of Mexico estuary to hypoxia: An analysis using box models. *Estuar. Coast. Shelf Sci.* **2007**, *74* (1−2), 239−253.
(10) Pokryfki, L.; Randall, R. E. Nearshore Hypoxia in the Bottom Water of the Northwestern Gulf of Mexico from 1981 to 1984. *Mar. Environ. Res.* **1987**, *22* (1), 75−90.
(11) Bahner, L. *User Guide for the Chesapeake Bay and Tidal Tributary Interpolator*; NOAA Chesapeake Bay Office: Annapolis, MD, 2006.
(12) Schwarz, G. Estimating Dimension of a Model. *Ann. Stat.* **1978**, *6* (2), 461−464.
(13) Mueller, K. L.; Yadav, V.; Curtis, P. S.; Vogel, C.; Michalak, A. M., Attributing the variability of eddy-covariance CO_2 flux measurements across temporal scales using geostatistical regression for a mixed northern hardwood forest. *Global Biogeochem. Cycles* **2010**, *24*.
(14) Obenour, D. R.; Michalak, A. M.; Zhou, Y.; Scavia, D. Quantifying the Impacts of Stratification and Nutrient Loading on Hypoxia in the Northern Gulf of Mexico. *Environ. Sci. Technol.* **2012**, *46* (10), 5489−5496.
(15) Chiles, J. P.; Delfiner, P. *Geostatistics: Modeling Spatial Uncertainty*; Wiley: New York, 1999.
(16) Great Lake National Program Office (GLNPO). http://cdx.epa.gov/ (accessed December 2008).
(17) Esterby, S. R.; Bertram, P. E. Compatibility of Sampling and Laboratory Procedures Evaluated for the 1985 3-Ship Intercomparison Study on Lake Erie. *J. Great Lakes Res.* **1993**, *19* (2), 400−417.
(18) Hawley, N.; Johengen, T. H.; Rao, Y. R.; Ruberg, S. A.; Beletsky, D.; Ludsin, S. A.; Eadie, B. J.; Schwab, D. J.; Croley, T. E.; Brandt, S. B. Lake Erie hypoxia prompts Canada-U.S. study. *EOS Trans. AGU* **2006**, *87* (32), 313.
(19) Bertram, P. E. Total Phosphorus and Dissolved-Oxygen Trends in the Central Basin of Lake Erie, 1970−1991. *J. Great Lakes Res.* **1993**, *19* (2), 224−236.
(20) National Geophysical Data Center. http://www.ngdc.noaa.gov/ (accessed November 2008).
(21) NASA Ocean Color Web facility. http://oceancolor.gsfc.nasa.gov/ (accessed November 2008).
(22) Great Lakes Surface Environmental Analysis (GLSEA). http://coastwatch.glerl.noaa.gov/glsea/ (accessed November 2008),
(23) Schwab, D. J.; Leshkevich, G. A.; Muhr, G. C. Automated mapping of surface water temperature in the Great Lakes. *J. Great Lakes Res.* **1999**, *25* (3), 468−481.
(24) Arthern, R. J.; Winebrenner, D. P.; Vaughan, D. G. Antarctic snow accumulation mapped using polarization of 4.3-cm wavelength microwave emission. *J. Geophys. Res., [Atmos.]* **2006**, *111* (D6), D06107 DOI: 10.1029/2004JD005667.
(25) Erickson, T. A.; Williams, M. W.; Winstral, A. Persistence of topographic controls on the spatial distribution of snow in rugged mountain terrain, Colorado, United States. *Water Resour. Res.* **2005**, *41* (4), W04014 DOI: 10.1029/2003WR002973.
(26) Haylock, M. R.; Hofstra, N.; Tank, A. M. G. K.; Klok, E. J.; Jones, P. D.; New, M. A European daily high-resolution gridded data set of surface temperature and precipitation for 1950−2006. *J. Geophys. Res., [Atmos.]* **2008**, *113* (D20), D20119 DOI: 10.1029/2008JD010201.
(27) Jerrett, M.; Burnett, R. T.; Kanaroglou, P.; Eyles, J.; Finkelstein, N.; Giovis, C.; Brook, J. R. A GIS- environmental justice analysis of particulate air pollution in Hamilton, Canada. *Environ. Plan. A* **2001**, *33* (6), 955−973.
(28) Murphy, R. R.; Curriero, F. C.; Ball, W. P. Comparison of Spatial Interpolation Methods for Water Quality Evaluation in the Chesapeake Bay. *J. Environ. Eng.-ASCE* **2010**, *136* (2), 160−171.
(29) Bogaert, P.; Russo, D. Optimal spatial sampling design for the estimation of the variogram based on a least squares approach. *Water Resour. Res.* **1999**, *35* (4), 1275−1289.
(30) Rao, Y. R.; Hawley, N.; Charlton, M. N.; Schertzer, W. M. Physical processes and hypoxia in the central basin of Lake Erie. *Limnol. Oceanogr.* **2008**, *53* (5), 2007−2020.
(31) Anderson, D. R.; Burnham, K. P.; White, G. C. Comparison of Akaike information criterion and consistent Akaike information criterion for model selection and statistical inference from capture-recapture studies. *J. Appl. Stat.* **1998**, *25* (2), 263−282.
(32) Gutjahr, A.; Bullard, B.; Hatch, S.; Hughson, L. Joint Conditional Simulations and the Spectral Approach for Flow Modeling. *Stochastic Hydrol. Hydraul.* **1994**, *8* (1), 79−108.
(33) Kitanidis, P. K. Quasi-Linear Geostatistical Theory for Inversing. *Water Resour. Res.* **1995**, *31* (10), 2411−2419.
(34) Michalak, A. M.; Bruhwiler, L.; Tans, P. P. A geostatistical approach to surface flux estimation of atmospheric trace gases. *J. Geophys. Res., [Atmos.]* **2004**, *109* (D14), D14109 DOI: 10.1029/2003JD004422.
(35) Kitanidis, P. K. Analytical expressions of conditional mean, covariance, and sample functions in geostatistics. *Stochastic Hydrol. Hydraul.* **1996**, *10* (4), 279−294.
(36) Loewen, M. R.; Ackerman, J. D.; Hamblin, P. F. Environmental implications of stratification and turbulent mixing in a shallow lake basin. *Can. J. Fish. Aquat. Sci.* **2007**, *64* (1), 43−57.
(37) Schertzer, W. M.; Saylor, J. H.; Boyce, F. M.; Robertson, D. G.; Rosa, F. Seasonal Thermal Cycle of Lake Erie. *J. Great Lakes Res.* **1987**, *13* (4), 468−486.
(38) Walker, N. D.; Rabalais, N. N. Relationships among satellite chlorophyll a, river inputs, and hypoxia on the Louisiana continental shelf, gulf of Mexico. *Estuaries Coasts* **2006**, *29* (6B), 1081−1093.
(39) Witter, D. L.; Ortiz, J. D.; Palm, S.; Heath, R. T.; Budd, J. W. Assessing the application of SeaWiFS ocean color algorithms to Lake Erie. *J. Great Lakes Res.* **2009**, *35* (3), 361−370.
(40) Makarewicz, J. C.; Bertram, P. Evidence for the Restoration of the Lake Erie Ecosystem - Water-Quality, Oxygen Levels, and Pelagic Function Appear to Be Improving. *Bioscience* **1991**, *41* (4), 216−223.
(41) Dolan, D. M. Point-Source Loadings of Phosphorus to Lake Erie - 1986−1990. *J. Great Lakes Res.* **1993**, *19* (2), 212−223.
(42) Vanderploeg, H. A.; Johengen, T. H.; Liebig, J. R. Feedback between zebra mussel selective feeding and algal composition affects mussel condition: Did the regime changer pay a price for its success? *Freshw. Biol.* **2009**, *54* (1), 47−63.

■ NOTE ADDED AFTER ASAP PUBLICATION

There was an error in the *y*-axis of Figure 1 of the version of this paper published January 3, 2013. The correct version published January 15, 2013.